MR image reconstruction based on densely connected residual generative adversarial network–DCR-GAN*

Amir Aghabiglou[1][0000−0001−6024−649X] and
Ender M. Eksioglu[2][0000−0002−7869−4159]

[1] Graduate School, Istanbul Technical University, Istanbul, Turkey
aghabaiglou17@itu.edu.tr
[2] Electronics and Communication Engineering Department, Istanbul Technical University, Istanbul, Turkey
eksioglue@itu.edu.tr

Abstract. Magnetic Resonance Image (MRI) reconstruction from undersampled data is an important ill-posed problem for biomedical imaging. For this problem, there is a significant tradeoff between the reconstructed image quality and image acquisition time reduction due to data sampling. Recently a plethora of solutions based on deep learning have been proposed in the literature to reach improved image reconstruction quality compared to traditional analytical reconstruction methods. In this paper, a novel densely connected residual generative adversarial network (DCR-GAN) is being proposed for fast and high-quality reconstruction of MR images. DCR blocks enable the reconstruction network to go deeper by preventing feature loss in the sequential convolutional layers. DCR block concatenates feature maps from multiple steps and gives them as the input to subsequent convolutional layers in a feed-forward manner. In this new model, the DCR block's potential to train relatively deeper structures is utilized to improve quantitative and qualitative reconstruction results in comparison to the other conventional GAN-based models. We can see from the reconstruction results that the novel DCR-GAN leads to improved reconstruction results without a significant increase in the parameter complexity or run times.

Keywords: Magnetic resonance imaging · MR Image Reconstruction · Deep learning · Densely Connected Residual Network.

1 Introduction

Magnetic resonance (MR) imaging is one of the key non-invasive modalities among clinical imaging techniques due to its ability to acquire high-contrast images from soft tissues. Despite its popularity, MR imaging is a rather lengthy process, and it is sensitive to motion [4]. This long image acquisition time makes

* This work is supported by TUBITAK (The Scientific and Technological Research Council of Turkey) under project no. 119E248.

MRI susceptible to motion artifacts like ghosting and blurring because of possible motions originated from patient discomfort. Any motion during the MRI phase encoding causes ill-matching in the spatial domain [23]. Shortening the MR imaging time is one of the effective solutions for this problem. Recently, deep learning (DL) models proved their capability for solving different image processing problems [3]. In this regard, deep learning based methods [13, 1, 6, 20, 8, 12] came to be an antidote for this issue. Through this path, the deep learning methods are trained using an undersampled dataset. Generative adversarial networks (GANs) as a particular DL framework have presented superb performance in imaging inverse problems in recent literature [7].

2 Related Works

GAN models predict the generative framework through an adversarial pipeline. GAN trains two networks at the same time in parallel. In MR image reconstruction, as shown in Fig. 1 the generative model G tries to reconstruct high-quality images while the discriminative network D predicts if the result is a ground truth image or it is a reconstructed one. In another point of view, G gives its best to reconstruct such a unique duplicate of a real image that fool D and push it to make mistake and accept the generator result as real one. GAN-based frameworks are proved their potential to predict undersampled k-space data and reconstruct high-resolution images [18].

In [21] a deep de-aliasing GAN has been proposed for reconstructing MR images. In DAGAN, a U-Net structure was used as the generator network [21] and the VGG (Visual Geometry Group) [19] perceptual loss was used alongside generative loss. TM Quan *et al* [16] deployed cyclic loss in residual GAN for MR image reconstruction under name of RefineGAN. In a study, CS-based GAN (GANCS) has been provided by Mardani *et al* [14] for MRI reconstruction. Coupling perceptual loss, pixel-wise, and the cyclic data consistency loss can improve the GAN-based model's performance for image synthesis [2]. Synthesis accuracy can be enriched using information from cross-section neighbors in each volume [2]. Recently, deep networks gained attention due to their promising performance but as they get deeper, their training becomes more challenging. They need more connections to prevent feature loss and gradient vanishment [10]. To address this drawback, layers during training can be referenced to the input layer by adding them together [9]. Huang *et al* [11] has been demonstrated that employing dense connections among layers can prevent gradient vanishing. Dense connections concatenate receptive fields step by step from all convolutional layers and feed them into the subsequent layer as an input [11]. Then, these residual and dense connections were proved their capacity in various image processing problems. In RDN [25] residual and densely connected networks are coupled together for image restoration. In a study, dense connections are applied to a U-Net based network for image denoising problems [15]. In the MR image segmentation study, the dense connections were added into the U-Net downsampling and upsampling stages [22]. Recently, a wide multimodal dense

U-Net has been put forward for reconstructing MR images related to patients who suffer from MS disease [5].

Getting inspired from the vantage points of both GAN-based and densely connected networks, we couple DCR blocks into the generative network. To the best of our knowlede, this is the the first time a DCR-GAN structure is being used for MR image reconstruction. The deep networks are applied on initial zero-filling (ZF) image estimates. The ZF images are generated directly from the undersampled k-space data via inverse DFT. For the k-space undersampling we utilize randomized Cartesian mask functions with 4-fold and 8-fold acceleration factors. In this regard, initially we developed a GAN (Fig. 1) using standard CNN with five convolutional layers as the generator (Fig. 2) and a binary classifier

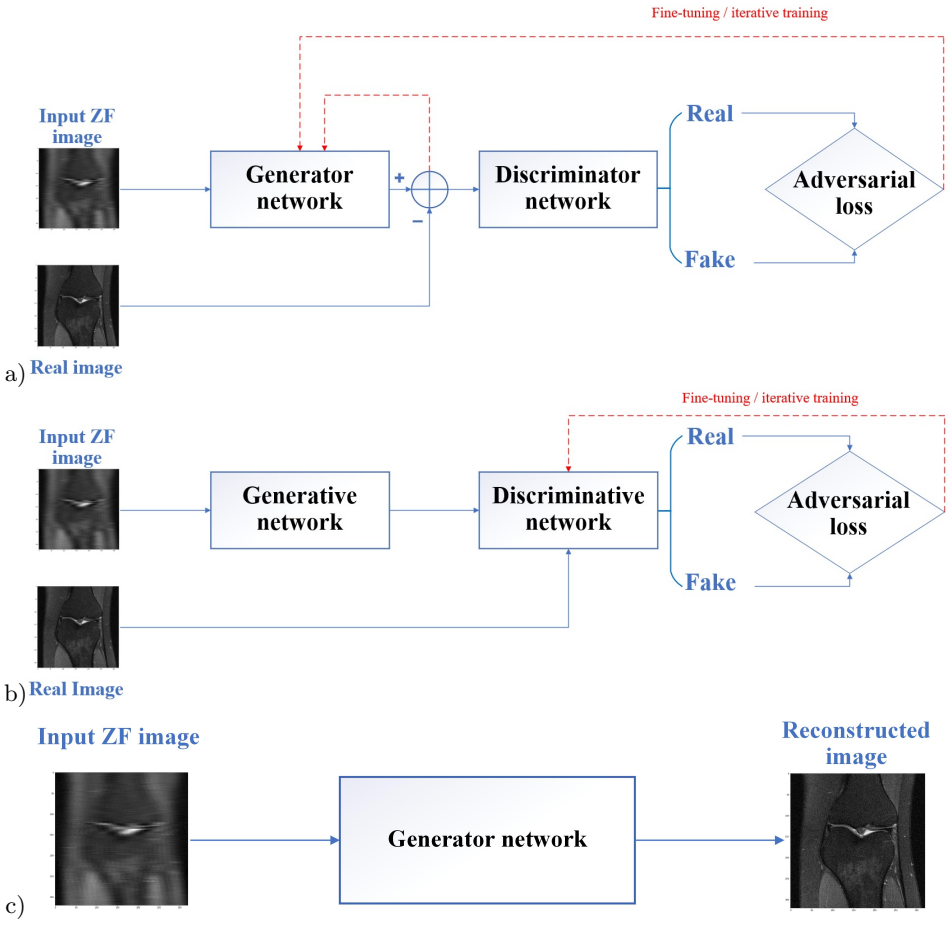

Fig. 1. GAN structure: a) Generator network during training step, b) Discriminator network during training step, c) Test step.

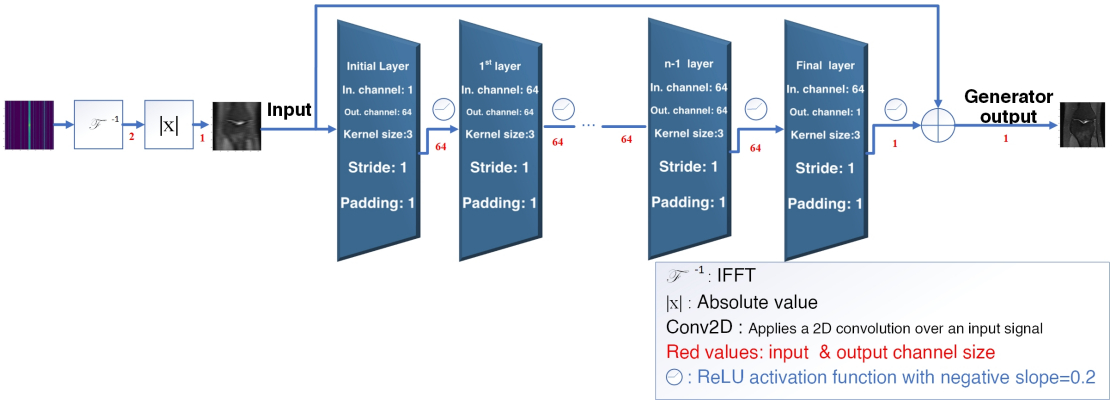

Fig. 2. Generative network architecture based on conventional CNN.

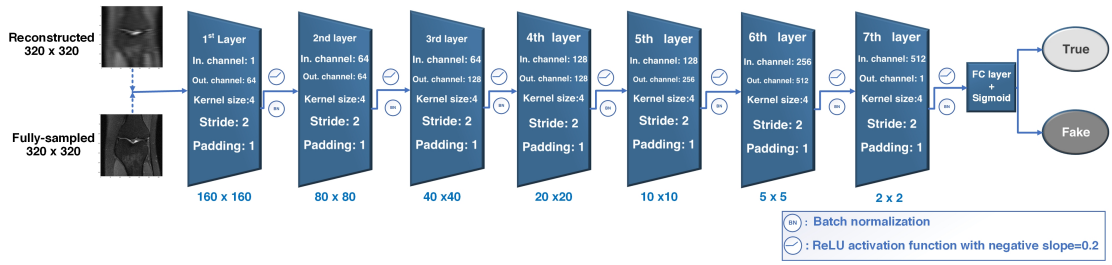

Fig. 3. Discriminator network architecture.

CNN as shown in Fig. 3 as the discriminator. We also adopted a VGG loss inside the generator loss. Secondly, we develop a densely connected residual GAN (DCR-GAN) and conduct qualitative and quantitative performance comparisons between these models. In this study, we have used the fastMRI challenge dataset of [24] for both training and testing purposes.

The rest of this article is arranged as follows. In Section 3, the general framework for MR image reconstruction and proposed structures are illustrated in detail. Moreover, in this section the developed network architectures are presented. In Section 4, qualitative and quantitative reconstruction results are compared using various metrics. Sample reconstructed images for all compared networks are presented in the final part of this section. In the last section, the contributions of the presented work are summarized and future research directions are given.

3 Proposed Approach

3.1 General Framework

The deep learning models reconstruct MR images by learning from the difference between ZF and ground truth images. In this regard, the fully-sampled data are undersampled in the spatial domain (x_{zf}) through a preprocessing step, then they are transported to the image domain using Inverse Fast Fourier transform (IFFT):

$$y = \mathscr{F}_{\Omega} x_{orig} \tag{1}$$

$$x_{zf} = \mathscr{F}^{-1} y \tag{2}$$

Here y is the undersampled data (observed data) in the k-space domain. $\mathscr{F}_{\Omega}$ indicates the undersampled Fourier transform function, $\mathscr{F}^{-1}$ is the IFFT, and x_{orig} shows the real image. MR image reconstruction model tries to complete missing points in input undersampled k-space data. This model tries to learn in the training step by minimizing the error between reconstructed image $\widetilde{x}$ and desired output. In another word, the goal is to find the best E function that minimizes the cost. So, the training process corresponds to the following optimization problem:

$$\widetilde{x} = E(x_{zf}) \tag{3}$$

$$\underset{\theta}{\operatorname{argmin}} \sum_{i=0}^{n_{data}} \|E_{\theta}(\widetilde{x}^{(i)} - x^{(i)})\| \tag{4}$$

Here, n_{data} refers to the number of training slices, and i is the image slice index. $E_{\theta}(x)$ denotes the network function, where θ represents the parameters of the underlying deep network model.

3.2 Proposed DCR-GAN

As shown in Fig. 1 the ZF images go into the proposed GAN. In general, GAN pipeline includes two competing networks, a generator (G) and a discriminator (D), with training parameters θ_G and θ_D, respectively. G should create fake images which must not be recognizable from ground truth images. To achieve this goal, network D help network G by classifying between fake and real images. Basically, this binary classifier for real samples gives value $D(x_{orig}) = 1$ and for fake data $(\widetilde{x}) = 0$. In mathematical terms, D and G play a two-player minimax game which is summarized in the following function:

$$\underset{G}{min}\underset{D}{max} V(D,G) = \mathbb{E}_{x\sim p_{data}}(x)[log(D(x))] + \mathbb{E}_{z\sim p_z}(Z)[1 - log(D(G(z)))] \tag{5}$$

Here, x indicates a sample slice from the fully sampled dataset distribution, and z is a sample image from ZF image distribution. Eq. 5 can be optimized

by training D to maximize the possibility of correct labeling, while G tries to minimize $log(1 - D(G(z)))$ and deceive D to accept the generated image as a real one. In this study, content loss was applied for generator network training. To this end, VGG loss is appended to the mean absolute error.

$$\mathcal{L}_{Total} = \alpha \mathcal{L}_{MAE} + \beta \mathcal{L}_{VGG} + \mathcal{L}_{GEN_{adv}} \tag{6}$$

$$\underset{\theta_G}{min} \mathcal{L}_{MAE}(\theta_G) = \|x_{orig} - \widetilde{x}\| \tag{7}$$

$$\underset{\theta_G}{min} \mathcal{L}_{VGG}(\theta_G) = \frac{1}{2} \|f_{vgg}(x_{orig}) - f_{vgg}(\widetilde{x})\|_2^2 \tag{8}$$

Here, f_{vgg} denotes the end-to-end function related to the pretrained VGG network. The generator adversarial loss is defined as follows.

$$\underset{\theta_G}{min} \mathcal{L}_{GEN_{adv}}(\theta_G) = -\log\left(D_{\theta_D}(G_{\theta_G}(x_{zf}))\right) \tag{9}$$

In this study, as in [21] the experimental hyperparameters α and β are set to 15 and 0.025, respectively. Here, we also applied data consistency (DC) layer [1] to improve our reconstruction results. DC layer can be defined as below:

$$x_{out} = \mathscr{F}^{-1}\left\{\overline{M} \circ (\mathscr{F}\widetilde{x}) + y\right\} \tag{10}$$

In Eq. 10, $\overline{M}$ designates the complement of the mask function used for undersampling the fully-sampled data. Here, $\circ$ is the point-wise multiplication operator, and y is defined through (1).

3.3 Architecture

The GAN model for MR reconstruction is provided in Fig. 1. As shown in Fig. 2, the generator pipeline includes five convolutional layers with the same training parameters as proposed in [17]. The discriminator network is shown in Fig. 3 and is similar to the one which is offered in [18]. This binary classifier includes 7 convolution layers that are followed by leaky-ReLU activation functions and end with a fully-connected layer. In DCR-GAN, initially the generator convolves the single channel ZF image into 64 feature-map, just like the plain CNN. Then these feature-maps are directed through three succeeding DCR blocks. The details of the DCR block can be seen in Fig. 4. In the final step, the single channel grayscale image is reconstructed through a reconstruction layer. The overall DCR-GAN generator network is seen in Fig. 5. Finally, a DC layer [1] can be applied to the resulting image to improve the reconstruction results.

4 Experimental Results

4.1 Quantitative Results

In this study, we developed a novel GAN based structure for MR image reconstruction. We have trained the proposed models using the fastMRI dataset [24].

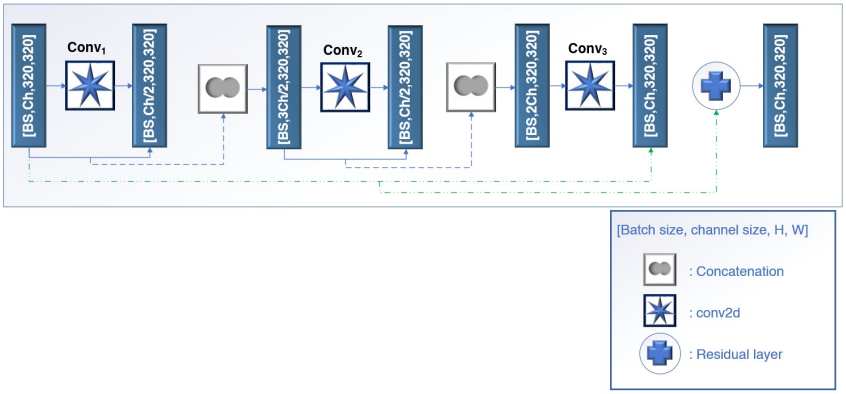

Fig. 4. DCR block structure.

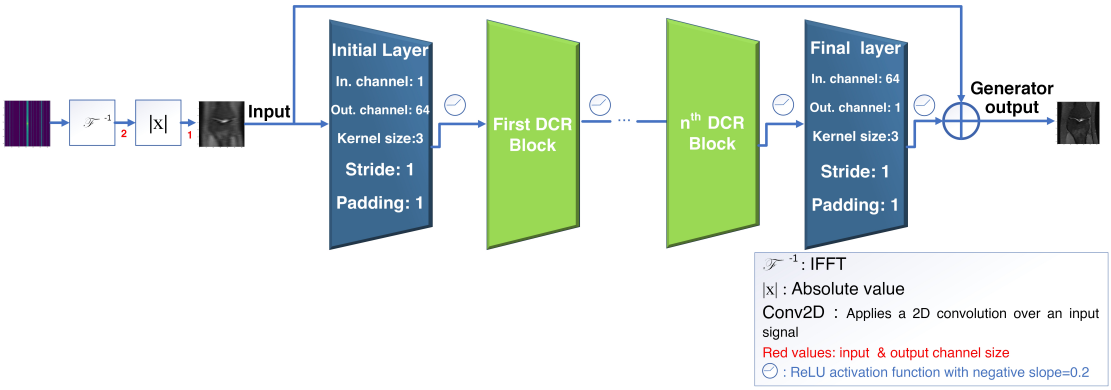

Fig. 5. Structure of the novel generator network with n DCR blocks.

The details for the dataset are provided in Table 1. The fully-sampled k-space is undersampled using random mask function with 4-fold and 8-fold acceleration factors. The simulation results are summarized in Table 2 for both undersampling acceleration factors. In Table 2, we have evaluated the proposed models performance using three popular performance metrics, namely Normalized Mean Squared Error (NMSE), Peak Signal to Noise Ratio(PSNR) and Structural Similarity Index Measure (SSIM) [8]. We did not utilize the VGG loss while training the DCR-GAN. Despite this factor, the proposed structure achieved promising results in terms of all three performance indices. In Table 2, the reconstruction time is provided for 32 test image slices. The required reconstruction times indicate that these methods are suitable for real-time clinical practice.

Table 1. Number of image volumes and image slices in the fastMRI single-coil dataset [24].

Subset name	Volumes	Slices
Training	973	34742
Validation	199	7135
Test	108	3903
Challenge	92	3305

Table 2. Simulation results for various models undersampled by 4-fold and 8-fold acceleration factor.

Acceleration	**4-fold**				**8-fold**				**Time (s)**
Network	**Loss**	**NMSE**($\times 10^{-3}$)	**SSIM**($\times 10^{-3}$)	**PSNR**	**Loss**	**NMSE**($\times 10^{-3}$)	**SSIM**($\times 10^{-3}$)	**PSNR**	
ZF	-	41.679	711.59	29.876	-	77.751	603.37	26.921	-
GAN	0.308	34.317	755.26	30.894	0.451	69.212	637.63	27.466	0.098
GAN with VGG	0.308	34.152	755.92	30.908	0.451	69.218	639.12	27.474	0.10
GAN with VGG +DC	0.307	33.176	751.53	31.085	0.449	66.206	634.15	27.671	0.10
GAN with 3 DCR	0.297	31.273	766.34	31.413	0.432	62.106	651.63	27.972	0.29
GAN with 3 DCR +DC	0.299	30.925	759.57	31.501	0.432	59.189	643.37	28.208	0.30

4.2 Qualitative Results

In this section, the reconstructed images for all the realized methods for a particular test sample are visualized. The performance of the proposed networks is evaluated by comparing the quality of these output reconstructed images. Fig. 6 depicts the original image, the ZF images (undersampled data with 4-fold and 8-fold acceleration factors), resulting images for Conventional GAN and the proposed networks. As shown in Fig. 6 the baseline GAN has not fully recovered the details while the proposed networks reconstructed images have better perceptual quality, and they have restored more detail and patterns. Moreover, the proposed structures resulting images have less severe artifacts, and most of the blurring defects have been removed. The quantitative results provided in Table 2 confirm the reconstructed images which are provided in Fig. 6.

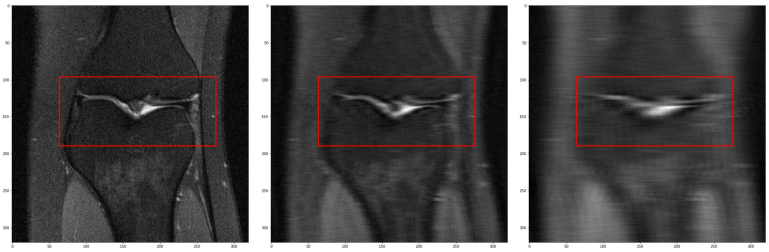

Ground truth image 4-fold zero-filling image 8-fold zero-filling image

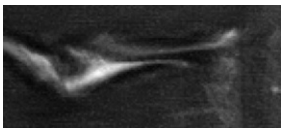

4-fold GAN

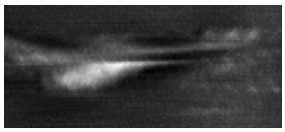

8-fold GAN

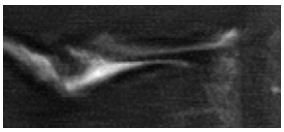

4-fold GAN with VGG loss

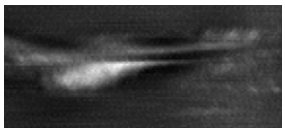

8-fold GAN with VGG loss

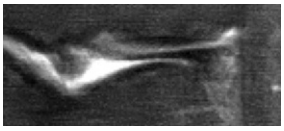

4-fold GAN with VGG loss + DC layer

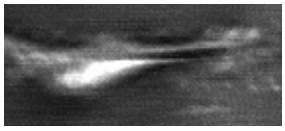

8-fold GAN with VGG loss + DC layer

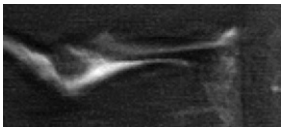

4-fold DCR-GAN with 3 DCR block

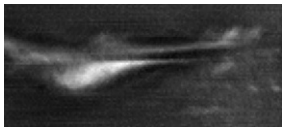

8-fold DCR-GAN with 3 DCR block

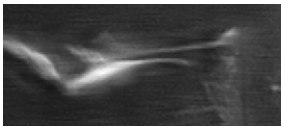

4-fold DCR-GAN with 3 DCR block + DC layer

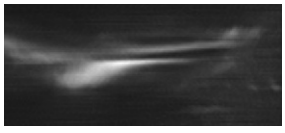

8-fold DCR-GAN with 3 DCR block + DC layer

Fig. 6. Reconstructed images for 4-fold and 8-fold undersampling with random mask function.

5 Conclusion

Recently, densely connected deep residual networks have shown their capacity for improving performance results in various image processing problems. Inspired by this fact, in this work dense connections are applied inside a generative adversarial network for MR image reconstruction. Appending DCR blocks to the generative network improves the qualitative and quantitative reconstruction results of the plain CNN based generator structure. We conducted simulations comparing the quantitative and qualitative performance results for the proposed structure and other methods from literature. Results reveal that in MR image reconstruction, the proposed DCR-GAN can compete with potent models from the literature. DCR-GAN with just three DCR blocks inside the generative network can get promising results for both 4-fold acceleration factor and the more aggressive 8-fold acceleration factor. In future work, DCR-GAN can get deepened using more DCR blocks. The DCR blocks may also get utilized in conjunction with more challenging generator structures, incorporating possibly U-Net based models or cascade network structures.

Acknowledgment

This work is supported by TUBITAK (The Scientific and Technological Research Council of Turkey) under project no. 119E248.

References

1. D. Kocanaogullari and E. M. Eksioglu: Deep Learning for MRI Reconstruction Using a Novel Projection Based Cascaded Network. In: 2019 IEEE 29th International Workshop on Machine Learning for Signal Processing (MLSP) (Oct 2019)
2. Dar, S.U., Yurt, M., Karacan, L., Erdem, A., Erdem, E., Çukur, T.: Image Synthesis in Multi-Contrast MRI With Conditional Generative Adversarial Networks. IEEE Transactions on Medical Imaging **38**(10), 2375–2388 (2019)
3. Eksioglu, E.M.: Decoupled algorithm for MRI reconstruction using nonlocal block matching model: BM3D-MRI. Journal of Mathematical Imaging and Vision **56**(3), 430–440 (2016)
4. Eksioglu, E.M., Tanc, A.K.: Denoising AMP for MRI Reconstruction: BM3D-AMP-MRI. SIAM Journal on Imaging Sciences **11**(3), 2090–2109 (2018)
5. Falvo, A., Comminiello, D., Scardapane, S., Scarpiniti, M., Uncini, A.: A Wide Multimodal Dense U-Net for Fast Magnetic Resonance Imaging. In: 2020 28th European Signal Processing Conference (EUSIPCO). pp. 1274–1278. IEEE (2021)
6. Ghodrati, V., Shao, J., Bydder, M., Zhou, Z., Yin, W., Nguyen, K.L., Yang, Y., Hu, P.: MR Image Reconstruction Using Deep Learning: Evaluation of Network Structure and Loss Functions. Quantitative Imaging in Medicine and Surgery **9**(9), 1516 (2019)
7. Goodfellow, I.J., Pouget-Abadie, J., Mirza, M., Xu, B., Warde-Farley, D., Ozair, S., Courville, A., Bengio, Y.: Generative Adversarial Networks. arXiv preprint arXiv:1406.2661 (2014)

8. Han, Y., Sunwoo, L., Ye, J.C.: k-Space Deep Learning for Accelerated MRI. IEEE Transactions on Medical Imaging **39**(2), 377–386 (2019)
9. He, K., Zhang, X., Ren, S., Sun, J.: Deep residual learning for image recognition. In: Proceedings of the IEEE Conference on Computer Vision and Pattern Recognition. pp. 770–778 (2016)
10. Hochreiter, S.: The vanishing gradient problem during learning recurrent neural nets and problem solutions. International Journal of Uncertainty, Fuzziness and Knowledge-Based Systems **06**(02), 107–116 (1998)
11. Huang, G., Liu, Z., Van Der Maaten, L., Weinberger, K.Q.: Densely connected convolutional networks. In: Proceedings of the IEEE Conference on Computer Vision and Pattern Recognition. pp. 4700–4708 (2017)
12. Hyun, C.M., Kim, H.P., Lee, S.M., Lee, S., Seo, J.K.: Deep learning for undersampled MRI reconstruction. Physics in Medicine & Biology **63**(13), 135007 (2018)
13. LeCun, Y., Bengio, Y., Hinton, G.: Deep learning. Nature **521**(7553), 436–444 (2015)
14. Mardani, M., Gong, E., Cheng, J.Y., Vasanawala, S.S., Zaharchuk, G., Xing, L., Pauly, J.M.: Deep Generative Adversarial Neural Networks for Compressive Sensing MRI. IEEE Transactions on Medical Imaging **38**(1), 167–179 (2019)
15. Park, B., Yu, S., Jeong, J.: Densely connected hierarchical network for image denoising. In: Proceedings of the IEEE/CVF Conference on Computer Vision and Pattern Recognition Workshops. pp. 0–0 (2019)
16. Quan, T.M., Nguyen-Duc, T., Jeong, W.K.: Compressed Sensing MRI Reconstruction Using a Generative Adversarial Network With a Cyclic Loss. IEEE Transactions on Medical Imaging **37**(6), 1488–1497 (2018)
17. Schlemper, J., Caballero, J., Hajnal, J.V., Price, A.N., Rueckert, D.: A Deep Cascade of Convolutional Neural Networks for Dynamic MR Image Reconstruction. IEEE Transactions on Medical Imaging **37**(2), 491–503 (2017)
18. Shaul, R., David, I., Shitrit, O., Riklin Raviv, T.: Subsampled brain MRI reconstruction by Generative Adversarial Neural networks. Medical Image Analysis **65**, 101747 (2020)
19. Simonyan, K., Zisserman, A.: Very deep convolutional networks for large-scale image recognition. arXiv preprint arXiv:1409.1556 (2014)
20. Wang, S., Su, Z., Ying, L., Peng, X., Zhu, S., Liang, F., Feng, D., Liang, D.: Accelerating magnetic resonance imaging via deep learning. In: 2016 IEEE 13th International Symposium on Biomedical Imaging (ISBI). pp. 514–517. IEEE (2016)
21. Yang, G., Yu, S., Dong, H., Slabaugh, G., Dragotti, P.L., Ye, X., Liu, F., Arridge, S., Keegan, J., Guo, Y., Firmin, D.: DAGAN: Deep De-Aliasing Generative Adversarial Networks for Fast Compressed Sensing MRI Reconstruction. IEEE Transactions on Medical Imaging **37**(6), 1310–1321 (2018)
22. Yuan, Y., Qin, W., Guo, X., Buyyounouski, M., Hancock, S., Han, B., Xing, L.: Prostate Segmentation with Encoder-Decoder Densely Connected Convolutional Network (Ed-Densenet). In: 2019 IEEE 16th International Symposium on Biomedical Imaging (ISBI 2019). pp. 434–437 (2019)
23. Zaitsev, M., Maclaren, J., Herbst, M.: Motion artifacts in MRI: A complex problem with many partial solutions. Journal of Magnetic Resonance Imaging **42**(4), 887–901 (2015)
24. Zbontar, J., Knoll, F., Sriram, A., Muckley, M.J., Bruno, M., Defazio, A., Parente, M., Geras, K.J., Katsnelson, J., Chandarana, H., et al.: fastMRI: An open dataset and benchmarks for accelerated MRI. arXiv preprint arXiv:1811.08839 (2018)

25. Zhang, Y., Tian, Y., Kong, Y., Zhong, B., Fu, Y.: Residual dense network for image restoration. IEEE Transactions on Pattern Analysis and Machine Intelligence **43**(7), 2480–2495 (2021)